

Color Image Segmentation for Medical Images using L*a*b* Color Space

Patel Janakkumar Baldevbhai¹, R. S. Anand²

¹Image & Signal Processing Group, Electrical Engineering Department, Research Scholar, EED, Indian Institute of Technology Roorkee, Uttarakhand, India.

²Electrical Engineering Department, Professor, EED, Indian Institute of Technology Roorkee, Uttarakhand, India

Abstract: Image segmentation is always a fundamental but challenging problem in computer vision. The simplest approach to image segmentation may be clustering of pixels. Our works in this paper address the problem of image segmentation under the paradigm of clustering. A robust clustering algorithm is proposed and utilized to do clustering on the L*a*b* color feature space of pixels. Image segmentation is straightforwardly obtained by setting each pixel with its corresponding cluster. We test our segmentation method on medical images and Mat lab standard images. The experimental results clearly show region of interest object segmentation.

Index Terms: color space, L*a*b* color space, color image segmentation, color clustering technique, medical image segmentation

I. Introduction

A Lab color space is a color-opponent space with dimension L for lightness and a and b for the color-opponent dimensions, based on nonlinearly compressed CIE XYZ color space coordinates. The coordinates of the Hunter 1948 L, a, b color space are L, a, and b [1][2]. However, Lab is now more often used as an informal abbreviation for the CIE 1976 (L*, a*, b*) color space (also called CIELAB, whose coordinates are actually L*, a*, and b*). Thus the initials Lab by themselves are somewhat ambiguous. The color spaces are related in purpose, but differ in implementation.

Both spaces are derived from the "master" space CIE 1931 XYZ color space, which can predict which spectral power distributions will be perceived as the same color, but which is not particularly perceptually uniform. Strongly influenced by the Munsell color system, the intention of both "Lab" color spaces is to create a space which can be computed via simple formulas from the XYZ space, but is more perceptually uniform than XYZ. Perceptually uniform means that a change of the same amount in a color value should produce a change of about the same visual importance. CIE L*a*b* (CIELAB) is the most complete color space specified by the International Commission on Illumination (Commission International d'Eclairage, hence its CIE initialism). It describes all the colors visible to the human eye and was created to serve as a device independent model to be used as a reference.

When storing colors in limited precision values, this can improve the reproduction of tones. Both Lab spaces are relative to the white point of the XYZ data they were converted from. Lab values do not define absolute colors unless the white point is also specified. Often, in practice, the white point is assumed to follow a standard and is not explicitly stated (e.g., for "absolute colorimetric" rendering intent ICC L*a*b* values are relative to CIE standard illuminant D50, while they are relative to the unprinted substrate for other rendering intents) [3]. Unlike the RGB and CMYK colour models, Lab colour is designed to approximate human vision. It aspires to perceptual uniformity, and its L component closely matches human perception of lightness. It can thus be used to make accurate colour balance corrections by modifying output curves in the a and b components, or to adjust the lightness contrast using the L component. In RGB or CMYK spaces, which model the output of physical devices rather than human visual perception, these transformations can only be done with the help of appropriate blend modes in the editing application.

Because Lab space is much larger than the gamut of computer displays, printers, or even human vision, a bitmap image represented as Lab requires more data per pixel to obtain the same precision as an RGB or CMYK bitmap. In the 1990s, when computer hardware and software was mostly limited to storing and manipulating 8 bit/channel bitmaps, converting an RGB image to Lab and back was a lossy operation. With 16 bit/channel support now common, this is no longer such a problem.

Colour spaces usually either model the human vision system or describe device dependent colour appearances. Although there exist many different colour spaces for human vision, those standardized by the CIE (i.e. XYZ, CIE Lab and CIE Luv, see for example Wyszecki & Stiles 2000) have gained the greatest popularity. These colour spaces are device independent and should produce colour constancy, at least in principle. Among device dependent colour spaces are HSI, NCC rgbI and YIQ (see Appendix 1 for formulae). The different versions of HS-spaces (HSI, HSV, Fleck HS and HSB) are related to the human vision system; they describe the colours in a way that is intuitive to humans.

Usually the output from CCD element is expressed as RGB values or corresponding values. This can be understood as a basic colour space from which the values are converted to the other device colour spaces. The RGB values are redundant and intensity dependent. Therefore, in many device colour spaces the intensity is separated from the chrominance. Use of only chrominance values offers robustness against changes in illumination intensity both in the time and spatial domains. A disadvantage is the loss of information related to different intensity levels of the same chrominance; in other words, for example black, grey and white cannot be separated by using only chromaticity values. It is interesting to note while the intensity may be the most significant feature in segmentation (Ohta *et al.* 1980), it is also the most sensitive component to changes in practical imaging conditions.

The values of device colour spaces can be converted to the corresponding values of a human colour space. For example, this transformation can be made by first selecting representative samples and calculating the transform matrix from them or by using the samples to train a neural network. The transform can be non-linear. The inputs (i.e. RGB) do not necessary have to be a 3x3 matrix; their values can be also obtained using polynomials with different degrees of polynomial. However, the created transform function depends heavily on the illumination conditions under which it was made. Therefore, the transform to human colour space still does not solve the colour constancy problem but alleviates the device dependency problem.

Additionally, many of the "colours" within Lab space fall outside the gamut of human vision, and are therefore purely imaginary; these "colours" cannot be reproduced in the physical world. Though colour management software, such as that built in to image editing applications, will pick the closest in-gamut approximation, changing lightness, colourfulness, and sometimes hue in the process, author Dan Margulis claims that this access to imaginary colours is useful, going between several steps in the manipulation of a picture [4]. CIE $L^*a^*b^*$ (CIELAB) is the most complete color space specified by the International Commission on Illumination (French *Commission Internationale de l'éclairage*, hence its CIE initialism). It describes all the colors visible to the human eye and was created to serve as a device independent model to be used as a reference.

The three coordinates of CIELAB represent the lightness of the color ($L^* = 0$ yields black and $L^* = 100$ indicates diffuse white; specular white may be higher), its position between red/magenta and green (a^* , negative values indicate green while positive values indicate magenta) and its position between yellow and blue (b^* , negative values indicate blue and positive values indicate yellow). The asterisk (*) after L , a and b are part of the full name, since they represent L^* , a^* and b^* , to distinguish them from Hunter's L , a , and b , described below.

Since the $L^*a^*b^*$ model is a three-dimensional model, it can only be represented properly in a three-dimensional space. Two-dimensional depictions are chromaticity diagrams: sections of the color solid with a fixed lightness. It is crucial to realize that the visual representations of the full gamut of colors in this model are never accurate; they are there just to help in understanding the concept.

Because the red/green and yellow/blue opponent channels are computed as differences of lightness transformations of (putative) cone responses, CIELAB is a chromatic value color space.

A related color space, the CIE 1976 (L^*, u^*, v^*) color space (a.k.a. CIELUV), preserves the same L^* as $L^*a^*b^*$ but has a different representation of the chromaticity components. CIELUV can also be expressed in cylindrical form (CIELCH), with the chromaticity components replaced by correlates of chroma and hue.

Since CIELAB and CIELUV, the CIE has been incorporating an increasing number of color appearance phenomena into their models, to better model color vision. These color appearance models, of which CIELAB, although not designed as [5] can be seen as a simple example [6], culminated with CIECAM02.

II. Color Space

The nonlinear relations for L^* , a^* , and b^* are intended to mimic the nonlinear response of the eye. Furthermore, uniform changes of components in the $L^*a^*b^*$ color space aim to correspond to uniform changes in perceived color, so the relative perceptual differences between any two colors in $L^*a^*b^*$ can be approximated by treating each color as a point in a three dimensional space (with three components: L^* , a^* ,

b*) and taking the Euclidean distance between them [7].

2.1 Devices-Independent Color Spaces

Some color spaces can express color in a device-independent way. Whereas RGB colors vary with display and scanner characteristics, and CMYK colors vary with printer, ink, and paper characteristics, device-independent colors are not dependent on any particular device and are meant to be true representations of colors as perceived by the human eye. These color representations, called device-independent color spaces, result from work carried out by the Commission Internationale d’Eclairage (CIE) and for that reason are also called CIE-based color spaces.

The most common method of identifying color within a color space is a three-dimensional geometry. The three color attributes, hue, saturation, and brightness, are measured, assigned numeric values, and plotted within the color space.

Table 1: Colour spaces

Base Space	Description	Derivative Space
CIEXYZ	Base CIE device-independent colour space	Colour spaces CIELAB
GRAY	Monochrome device-dependent colour space	----
RGB	Base additive device-dependent colour space	HLS, HSV
CMY	Base subtractive device-dependent colour space	CMYK

Conversion from an RGB color space to a CMYK color space involves a number of variables. The type of printer or printing press, the paper stock, and the inks used all influence the balance between cyan, magenta, yellow, and black. In addition, different devices have different gamuts, or ranges of colors that they can produce. Because the colors produced by RGB and CMYK specifications are specific to a device, they’re called device-dependent color spaces. Device color spaces enable the specification of color values that are directly related to their representation on a particular device.

Device-independent color spaces can be used as interchange color spaces to convert color data from the native color space of one device to the native color space of another device.

The CIE created a set of color spaces that specify color in terms of human perception. It then developed algorithms to derive three imaginary primary constituents of color—X, Y, and Z—that can be combined at different levels to produce all the color the human eye can perceive. The resulting color model, CIEXYZ, and other CIE color models form the basis for all color management systems. Although the RGB and CMYK values differ from device to device, human perception of color remains consistent across devices. Colors can be specified in the CIE-based color spaces in a way that is independent of the characteristics of any particular display or reproduction device. The goal of this standard is for a given CIE-based color specification to produce consistent results on different devices, up to the limitations of each device.

2.1.1 XYZ Space

There are several CIE-based color spaces, but all are derived from the fundamental XYZ space. The XYZ space allows colors to be expressed as a mixture of the three tristimulus values X, Y, and Z. The term tristimulus comes from the fact that color perception results from the retina of the eye responding to three types of stimuli. After experimentation, the CIE set up a hypothetical set of primaries, XYZ, that correspond to the way the eye’s retina behaves.

The CIE defined the primaries so that all visible light maps into a positive mixture of X, Y, and Z, and so that Y correlates approximately to the apparent lightness of a color. Generally, the mixtures of X, Y, and Z components used to describe a color are expressed as percentages ranging from 0 per cent up to, in some cases, just over 100 per cent.

Other device-independent color spaces based on XYZ space are used primarily to relate some particular aspect of color or some perceptual color difference to XYZ values.

2.1.2 Yxy Space

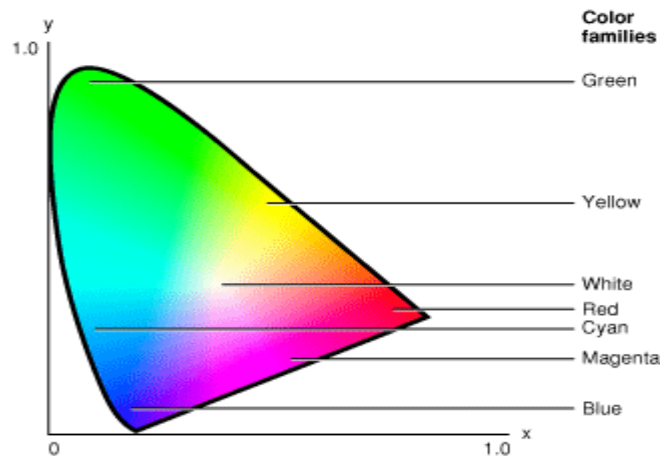
Yxy space expresses the XYZ values in terms of x and y chromaticity coordinates, somewhat analogous to the hue and saturation coordinates of HSV space. The coordinates are shown in the following formulas, used to convert XYZ into Yxy:

$$Y = Y$$

$$x = X / (X + Y + Z)$$

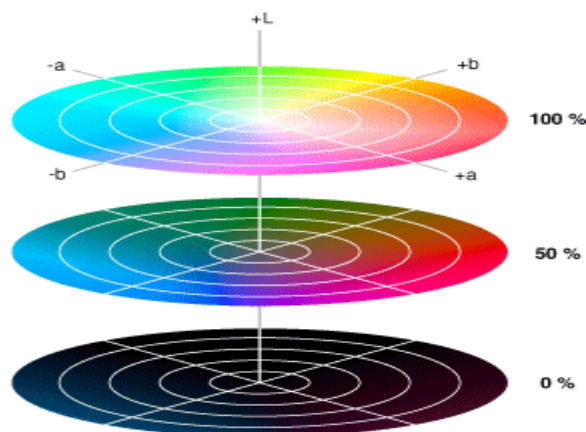
$$y = Y / (X + Y + Z)$$

Note that the Z tristimulus value is incorporated into the new coordinates and does not appear by itself. Since Y still correlates to the lightness of a color, the other aspects of the color are found in the chromaticity coordinates x and y. This allows color variation in Yxy space to be plotted on a two-dimensional diagram. Figure 2-5 shows the layout of colors in the x and y plane of Yxy space.



(a)

L*a*b* color space



(b)

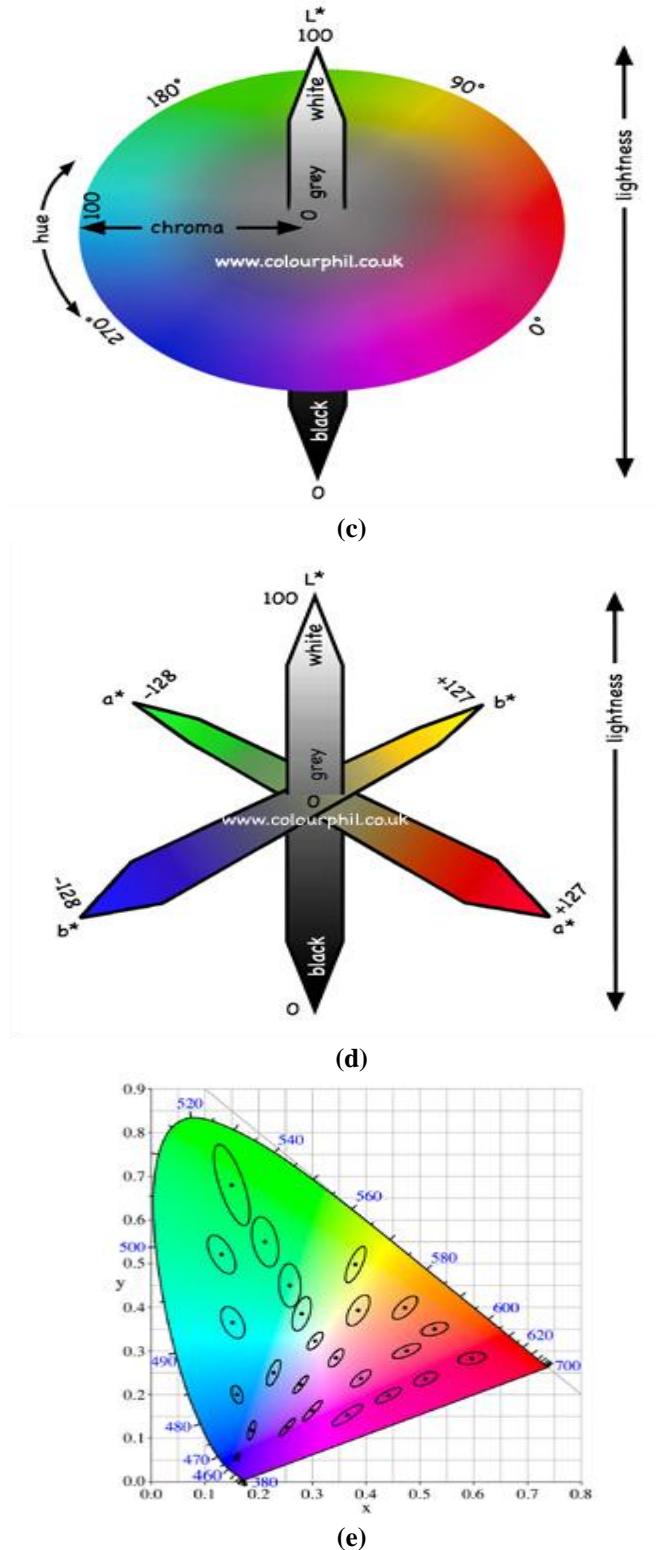


Figure 1: (a) Yxy chromaticity diagram in the CIE color space (b) $L^*a^*b^*$ color space (c) Hue, Chroma and L^* representation (d) $L^*a^*b^*$ representation (e) MacAdam diagram in the CIE 1931 color space

2.1.3 $L^*u^*v^*$ Space and $L^*a^*b^*$ Space

One problem with representing colors using the XYZ and Yxy color spaces is that they are perceptually nonlinear: it is not possible to accurately evaluate the perceptual closeness of colors based on their relative positions in XYZ or Yxy space. Colors that are close together in Yxy space may seem very different to observers, and colors that seem very similar to observers may be widely separated in Yxy space.

$L^*u^*v^*$ space and $L^*a^*b^*$ space are nonlinear transformations of the XYZ tristimulus space. These

spaces are designed to have a more uniform correspondence between geometric distances and perceptual distances between colors that are seen under the same reference illuminant. A rendering of L*a*b* space is shown in Figure 2-6.

Both L*u*v* space and L*a*b* space represent colors relative to a reference white point, which is a specific definition of what is considered white light, represented in terms of XYZ space, and usually based on the whitest light that can be generated by a given device.

Note: Because L*u*v* space and L*a*b* space represent colors relative to a specific definition of white light, they are not completely device independent; two numerically equal colors are truly identical only if they were measured relative to the same white point.

Measuring colors in relation to a white point allows for color measurement under a variety of illuminations. A primary benefit of using L*u*v* space and L*a*b* space is that the perceived difference between any two colors is proportional to the geometric distance in the color space between their color values, if the color differences are small. Use of L*u*v* space or L*a*b* space is common in applications where closeness of color must be quantified, such as in colorimetry, gemstone evaluation, or dye matching. The three coordinates of CIELAB represent the lightness of the color ($L^* = 0$ yields black and $L^* = 100$ indicates diffuse white; specular white may be higher), its position between red/magenta and green (a^* , negative values indicate green while positive values indicate magenta) and its position between yellow and blue (b^* , negative values indicate blue and positive values indicate yellow). The asterisk (*) after L, a and b are part of the full name, since they represent L^* , a^* and b^* , to distinguish them from Hunter's L, a and b. One of the most important attributes of the L*a*b*-model is the device independency.

2.1.4 Colour Spaces - CIE Lab & LCH

This is a very basic introduction to two related colour spaces which are becoming increasingly important in the world of colour reproduction. These are among the tristimulus (three-dimensional) colour spaces developed by the C.I.E.

C.I.E. is short for "Commission Internationale de l'Eclairage", which in English is the "International Commission on Illumination". A professional scientific organisation founded over 90 years ago to exchange information on "all matters relating to the science and art of lighting". The standards for colour spaces representing the visible spectrum were established in 1931, but have been revised more recently. For those of us involved in creating colour which will be reproduced on a printed page, it is easy to forget that there are other industries which need to describe colour! RGB or CMYK descriptions won't be of any use to paint or textile manufacturers! Terms such as "maroon" or "navy blue" won't be precise enough. There are many CIE colour spaces, more correctly known as models, which serve different purposes. They are all "device independent", unlike RGB or CMYK colour spaces which are related to a specific device (camera, scanner, or press, etc.) and/or material type (paper, ink set, film emulsion or lighting, etc.). These RGB and CMYK spaces usually do not cover the entire visible colour spectrum or gamut. The CIE also specify lighting conditions.

2.1.5 The CIE LCH Colour Space or Colour Model

This is possibly a little easier to comprehend than the Lab colour space, with which it shares several features. It is more correctly known as $L^*C^*H^*$. Essentially it is in the form of a sphere. There are three axes; L^* and C^* and H° . The L^* axis represents Lightness. This is vertical; from 0, which has no lightness (i.e. absolute black), at the bottom; through 50 in the middle, to 100 which is maximum lightness (i.e. absolute white) at the top.

The C^* axis represents Chroma or "saturation". This ranges from 0 at the centre of the circle, which is completely unsaturated (i.e. a neutral grey, black or white) to 100 or more at the edge of the circle for very high Chroma (saturation) or "colour purity".

If we take a horizontal slice through the centre, we see a coloured circle. Around the edge of the circle we see every possible saturated colour, or Hue. This circular axis is known as H° for Hue. The units are in the form of degrees $^\circ$ (or angles), ranging from 0° (red) through 90° (yellow), 180° (green), 270° (blue) and back to 0° .

The LCH colour model is very useful for retouching images in a colour managed workflow, using high-end editing or scanning applications. LCH is device-independent. A similar colour model is HSB or HSL for Hue, Saturation and brightness (lightness) which can be used in Adobe Photoshop and other applications. Technically this is "device-dependent", however it is particularly useful for editing RGB images. For example to edit a green: Adjust the Hue angle by increasing it to make it "bluish" or by reducing it to make it "yellowish"; Increase the Saturation (Chroma) to make it "cleaner"; increase the Brightness or Lightness to make it lighter.

2.1.6 The CIE Lab Colour Space or Colour Model

This is more correctly known as L*a*b*. Just as in LCH, the vertical L* axis represents "Lightness", ranging from 0-100. The other (horizontal) axes are now represented by a* and b*. These are at right angles to each other and cross each other in the centre, which is neutral (grey, black or white). They are based on the principal that a colour cannot be both red and green, or blue and yellow. The a* axis is green at one extremity (represented by -a), and red at the other (+a). The b* axis has blue at one end (-b), and yellow (+b) at the other.

The centre of each axis is 0. A value of 0 or very low numbers of both a* and b* will describe a neutral or near neutral. In theory there are no maximum values of a* and b*, but in practice they are usually numbered from -128 to +127 (256 levels).

CIE Lab is extensively used in many industries apart from printing and photography. Its uses include providing exact colour specifications for paint (including automotive, household, etc.), dyes (including textiles, plastics, etc.), printing ink and paper. Nowadays it is becoming of increasing importance in specifying printing standards such as in ISO-12647, where it is usually used instead of densitometry. For example "Paper Type 1" (115gsm gloss coated white, wood free) has "Paper Shade" described as "L* 95, a* 0, b* -2". So the L*95 is very light, the a*0 neutral, and the b*-2 very slightly "blueish". "Paper Type 5" (115gsm uncoated yellowish offset) is described as L* 90, a* 0, b* 9. So is a darker, more "yellow" paper. If you compare the different Lab values for Type 1 & 5 you will understand the descriptions. Lab measurements can be used to control printing, typically by monitoring a 3-colour neutral grey mid-tone patch. It is also very useful for specifying a spot colour, perhaps an important "house" or "corporate" colour such as "Coca-Cola Red". The same colour could be used for printed matter, vans, clothing, and buildings and of course tin cans.

In ICC Colour Management CIE Lab is often used as the Profile Connection Space (PCS) where it provides a link between two colour profiles, such as Input RGB (scanner or camera) and Output (CMYK or RGB press or inkjet). All ICC profiles contain a PCS. In an input profile the tables will convert the scanner's or camera's RGB space to the PCS (Lab). An output profile will convert the PCS (Lab) to the digital printer's or printing press's colour space (CMYK). The other PCS colour space is CIE XYZ, which is often also used by spectrophotometers

2.1.7 RGB and CMYK conversions

There are no simple formulas for conversion between RGB or CMYK values and L*a*b*, because the RGB and CMYK color models are device dependent. The RGB or CMYK values first need to be transformed to a specific absolute color space, such as sRGB or Adobe RGB. This adjustment will be device dependent, but the resulting data from the transform will be device independent, allowing data to be transformed to the CIE 1931 color space and then transformed into L*a*b*. The L* coordinate ranges from 0 to 100. The possible range of a* and b* coordinates is independent of the colour space that one is converting from, since the conversion below uses X and Y which come from RGB.

2.2 CIE XYZ to CIE L*a*b* (CIELAB) and CIELAB to CIE XYZ conversions

2.2.1 The forward transformation

$$L^* = 116f\left(\frac{Y}{Y_n}\right) - 16$$

$$a^* = 500\left[f\left(\frac{X}{X_n}\right) - f\left(\frac{Y}{Y_n}\right)\right]$$

$$b^* = 200\left[f\left(\frac{Y}{Y_n}\right) - f\left(\frac{Z}{Z_n}\right)\right]$$

Where,

$$f(t) = \begin{cases} t^{1/3} & \text{if } t > \left(\frac{6}{29}\right)^3 \\ \frac{1}{3}\left(\frac{29}{6}\right)^2 t + \frac{4}{29} & \text{otherwise} \end{cases}$$

Here X_n , Y_n and Z_n are the CIE XYZ tristimulus values of the reference white point (the subscript n suggests "normalized").

The division of the $f(t)$ function into two domains was done to prevent an infinite slope at $t = 0$. $f(t)$ was assumed to be linear below some $t = t_0$, and was assumed to match the $t^{1/3}$ part of the function at t_0 in both value and slope. In other words:

$$t_0^{1/3} = at_0 + b(\text{matchinvalue})$$

$$\frac{1}{3}t_0^{-2/3} = a(\text{matchinslope})$$

The slope was chosen to be $b = 16/116 = 4/29$. The above two equations can be solved for a and t_0 :

$$a = \frac{1}{3}\delta^{-2} = 7.787037\dots$$

$$t_0 = \delta^3 = 0.008856\dots$$

Where $\delta = 6/29$ [8]. Note that the slope at the join is $b = 4/29 = 2\delta/3$.

2.2.2 The reverse transformation

The reverse transformation is most easily expressed using the inverse of the function f above:

$$Y = Y_n f^{-1}\left(\frac{1}{116}(L^* + 16)\right)$$

$$X = X_n f^{-1}\left(\frac{1}{116}(L^* + 16) + \frac{1}{500}a^*\right)$$

$$Z = Z_n f^{-1}\left(\frac{1}{116}(L^* + 16) - \frac{1}{200}b^*\right)$$

Where,

$$f^{-1}(t) = \begin{cases} t^3 & \text{if } t > \frac{6}{29} \\ 3\left(\frac{6}{29}\right)^2\left(t - \frac{4}{29}\right) & \text{otherwise} \end{cases}$$

2.3 Lab Colour Space

The overall concept starting from conversion of original image to L*a*b* color space and then object segmentation is represented through block diagram in fig.2.

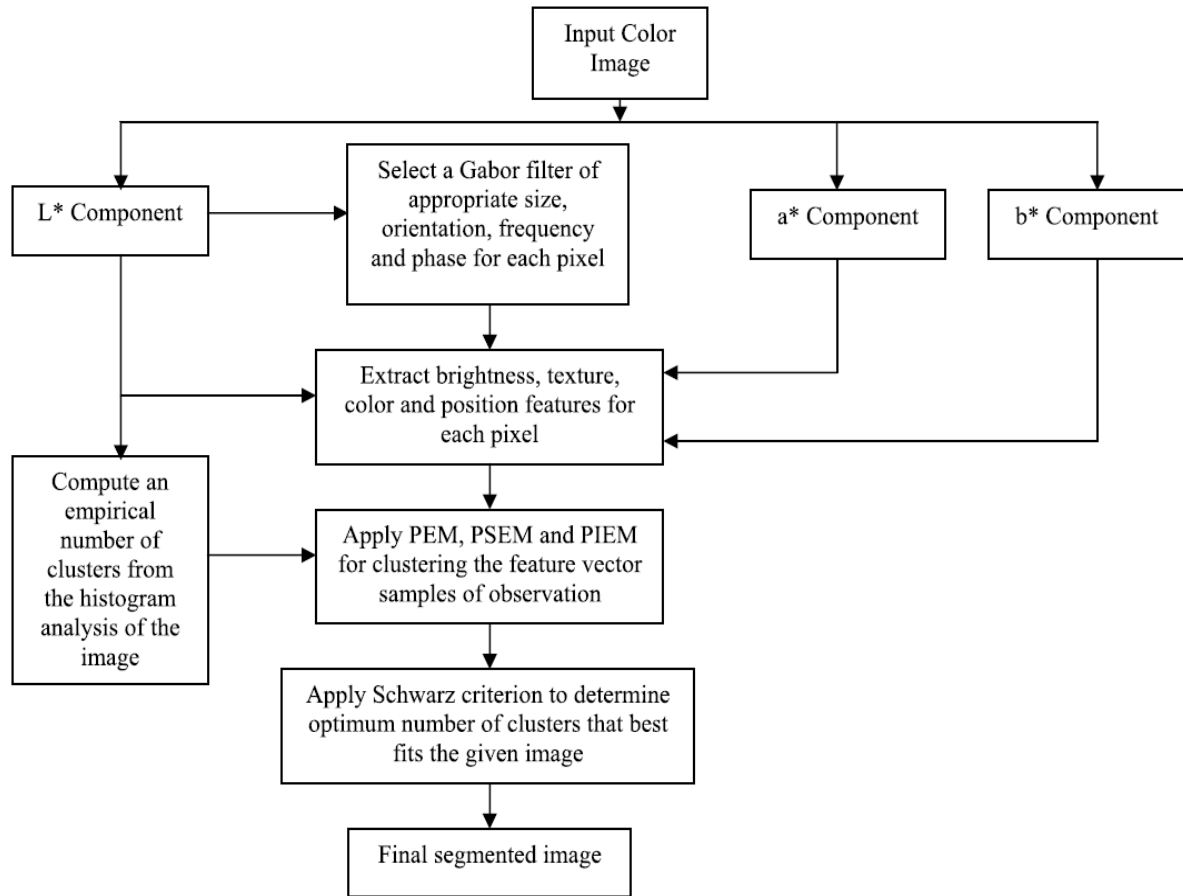


Fig. 2 Block Diagram representing usefulness of L*a*b* color space for color image segmentation.

L is a correlate of lightness, and is computed from the Y tristimulus value using Priest's approximation to Munsell value:

$$L = 100\sqrt{Y/Y_n}$$

Where, Y_n is the Y tristimulus value of a specified white object. For surface-colour applications, the specified white object is usually (though not always) a hypothetical material with unit reflectance and which follows Lambert's law. The resulting L will be scaled between 0 (black) and 100 (white); roughly ten times the Munsell value. Note that a medium lightness of 50 is produced by a luminance of 25, since

$$100\sqrt{25/100} = 100.1/2$$

a and b are termed opponent color axes. a represents, roughly, Redness (positive) versus Greenness (negative). It is computed as:

$$a = K_a \left(\frac{X/X_n - Y/Y_n}{\sqrt{Y/Y_n}} \right)$$

Where, K_a is a coefficient which depends upon the illuminant (for D65, K_a is 172.30; see approximate formula below) and X_n is the X tristimulus value of the specified white object. The other opponent colour axis, b, is positive for yellow colours and negative for blue colours. It is computed as:

$$b = K_b \left(\frac{Y/Y_n - Z/Z_n}{\sqrt{Y/Y_n}} \right)$$

Where, K_b is a coefficient which depends upon the illuminant (for D65, K_b is 67.20; see approximate formula below) and Z_n is the Z tristimulus value of the specified white object [9].

Both a and b will be zero for objects which have the same chromaticity coordinates as the specified white objects (i.e., achromatic, grey, objects).

2.3.1 Approximate formulas for K_a and K_b

In the previous version of the Hunter *Lab* colour space, K_a was 175 and K_b was 70. Apparently, Hunter Associates Lab discovered that better agreement could be obtained with other colour difference metrics, such as CIELAB (see above) by allowing these coefficients to depend upon the illuminants. Approximate formulas are:

$$K_a \approx \frac{175}{198.04}(X_n + Y_n)$$

$$K_b \approx \frac{70}{218.11}(Y_n + Z_n)$$

Which, result in the original values for Illuminant C, the original illuminant with which the *Lab* colour space was used.

2.3.2 Adams chromatic valence space

Adams chromatic valence colour spaces are based on two elements: A (relatively) uniform lightness scale and a (relatively) uniform chromaticity scale [10]. If we take as the uniform lightness scale Priest's approximation to the Munsell Value scale, which would be written in modern notation:

$$L = 100\sqrt{Y/Y_n}$$

and, as the uniform chromaticity coordinates:

$$C_a = \frac{X/X_n}{Y/Y_n} - 1 = \frac{X/X_n - Y/Y_n}{Y/Y_n}$$

$$C_b = k_e \left(1 - \frac{Z/Z_n}{Y/Y_n} \right) = k_e \frac{Y/Y_n - Z/Z_n}{Y/Y_n}$$

Where, k_e is a tuning coefficient, we obtain the two chromatic axes:

$$a = K.L.C_a = K.100 \frac{X/X_n - Y/Y_n}{\sqrt{Y/Y_n}}$$

And

$$b = K.L.C_b = K.100 k_e \frac{Y/Y_n - Z/Z_n}{\sqrt{Y/Y_n}}$$

Which, is identical to the Hunter *Lab* formulae given above if we select $K = K_a/100$ and $k_e = K_b/K_a$. Therefore, the Hunter *Lab* color space is an Adams chromatic valence color space.

2.4 Color difference

The difference or distance between two colours is a metric of interest in color science. It allows people to quantify a notion that would otherwise be described with adjectives, to the detriment of anyone whose work is color critical. Common definitions make use of the Euclidean distance in a device independent color space.

2.4.1 Delta E

The International Commission on Illumination (CIE) calls their distance metric ΔE^*_{ab} (also called ΔE^* , dE^* , dE , or "Delta E") where delta is a Greek letter often used to denote difference, and **E** stands for *Empfindung*; German for "sensation". Use of this term can be traced back to the influential Hermann von Helmholtz and Ewald Hering.

In theory, a ΔE of less than 1.0 is supposed to be indistinguishable unless the samples are adjacent to one another. However, perceptual non-uniformities in the underlying CIELAB color space prevent this and have led to the CIE's refining their definition over the years. These non-uniformities are important because the human eye is more sensitive to certain colours than others. A good metric should take this into account in order for the notion of a "just noticeable difference" to have meaning. Otherwise, a certain ΔE that may be insignificant between two colours that the eye is insensitive to may be conspicuous in another part of the spectrum [11]. Unit of measure that calculates and quantifies the difference between two colours -- one a reference colour, the other a sample colour that attempts to match it -- based on L*a*b* coordinates.

The "E" in "Delta E" comes from the German word "Empfindung," meaning "feeling, sensation." "Delta" comes from the Greek language, and is used in mathematics (as the symbol Δ) to signify an incremental change in a variable, i.e., a difference. So, "Delta E" comes to mean "a difference in sensation."

A Delta E of 1 or less between two colours that are not touching one another is barely perceptible by the average human observer; a Delta E between 3 and 6 is typically considered an acceptable match in commercial reproduction on printing presses. (Note: Human vision is more sensitive to colour differences if two colours actually touch each other.)

The higher the Delta E, the greater the difference between the two samples being compared. There are several methods by which to calculate Delta E values, the most common of which are Delta E 1976, Delta E 1994, Delta E CMC, and Delta E 2000. Delta E 2000 is considered to be the most accurate formulation to use for small delta E calculations (<5).

Daylight human vision (a.k.a., photopic vision) is most sensitive to the green region of the colour spectrum around 550nm, and least sensitive to colours near the extremes of the visible spectrum (deep blue-purples at one end and deep reds at the other). For that reason, colour differences in the latter regions are harder for the average human observer to detect and quantify, making Delta E measurements for those colours possibly less accurate.

2.4.2 CIE76

Using (L_1^*, a_1^*, b_1^*) and (L_2^*, a_2^*, b_2^*) two colours in L*a*b*:

$$\Delta E_{ab}^* = \sqrt{(L_2^* - L_1^*)^2 + (a_2^* - a_1^*)^2 + (b_2^* - b_1^*)^2}$$

$\Delta E_{ab}^* \approx 2.3$ corresponds to a JND (just noticeable difference) [12].

2.4.3 CIE94

The 1976 definition was extended to address perceptual non-uniformities, while retaining the L*a*b* color space, by the introduction of application-specific weights derived from an automotive paint test's tolerance data.

ΔE (1994) is defined in the L*C*h* color space with differences in lightness, chroma and hue calculated from L*a*b* coordinates. Given a reference color [13] (L_1^*, a_1^*, b_1^*) and another color (L_2^*, a_2^*, b_2^*) the difference is [14][15][16]:

$$\Delta E_{94}^* = \sqrt{\left(\frac{\Delta L^*}{K_L}\right)^2 + \left(\frac{\Delta C_{ab}^*}{1 + K_1 C_1^*}\right)^2 + \left(\frac{\Delta H_{ab}^*}{1 + K_2 C_1^*}\right)^2}$$

Where:

$$\begin{aligned} \Delta L^* &= L_1^* - L_2^* \\ C_1^* &= \sqrt{a_1^{*2} + b_1^{*2}} \\ C_2^* &= \sqrt{a_2^{*2} + b_2^{*2}} \end{aligned}$$

$$\Delta C_{ab}^* = C_1^* - C_2^*$$

$$\Delta H_{ab}^* = \sqrt{\Delta E_{ab}^{*2} - \Delta L^{*2} - \Delta C_{ab}^{*2}} = \sqrt{\Delta a^{*2} + \Delta b^{*2} - \Delta C^{*2}}$$

$$\Delta a^* = a_1^* - a_2^*$$

$$\Delta b^* = b_1^* - b_2^*$$

and where the weighting factors **K** depend on the application.

2.4.4 CIEDE2000

Since the 1994 definition did not adequately resolve the perceptual uniformity issue, the CIE refined their definition, adding five corrections [17]:

- A hue rotation term (R_T), to deal with the problematic blue region (hue angles in the neighbourhood of 275°);
- Compensation for neutral colours (the primed values in the L*C*h differences)
- Compensation for lightness (S_L)
- Compensation for chroma (S_C)
- Compensation for hue (S_H)

$$\Delta E_{00}^* = \sqrt{\left(\frac{\Delta L'}{S_L}\right)^2 + \left(\frac{\Delta C'}{S_C}\right)^2 + \left(\frac{\Delta H'}{S_H}\right)^2} + R_T \frac{\Delta C'}{S_C} \frac{\Delta H'}{S_H}$$

$$\Delta L' = L_2^* - L_1^*$$

$$\bar{L} = \frac{L_1^* + L_2^*}{2} \quad \bar{C} = \frac{C_1^* + C_2^*}{2}$$

$$a_1' = a_1 + \frac{a_1}{2} \left(1 - \sqrt{\frac{\bar{C}^7}{\bar{C}^7 + 25^7}}\right) \quad a_2' = a_2 + \frac{a_2}{2} \left(1 - \sqrt{\frac{\bar{C}^7}{\bar{C}^7 + 25^7}}\right)$$

$$\bar{C}' = \frac{C_1' + C_2'}{2} \quad \text{And} \quad \Delta C' = C_1' - C_2'$$

Where, $C_1' = \sqrt{a_1'^2 + b_1'^2}$ $C_2' = \sqrt{a_2'^2 + b_2'^2}$

$$h_1' = \tan^{-1} \left(\frac{b_1'}{a_1'} \right)_{\text{Mod } 2\pi}$$

$$h_2' = \tan^{-1} \left(\frac{b_2'}{a_2'} \right)_{\text{Mod } 2\pi}$$

$$\Delta h' = \begin{cases} h'_2 - h'_1 & |h'_1 - h'_2| \leq \pi \\ h'_2 - h'_1 + 2\pi & |h'_1 - h'_2| > \pi, h'_2 \leq h'_1 \\ h'_2 - h'_1 - 2\pi & |h'_1 - h'_2| > \pi, h'_2 > h'_1 \end{cases}$$

$$\Delta \bar{H}' = 2\sqrt{C'_1 C'_2} \sin\left(\frac{\Delta h'}{2}\right) \quad \bar{H}' = \begin{cases} \frac{(h'_1 + h'_2 + 2\pi)}{2} & |h'_1 - h'_2| > \pi \\ \frac{(h'_1 + h'_2)}{2} & |h'_1 - h'_2| \leq \pi \end{cases}$$

$$T = 1 - 0.17 \cos\left(\bar{H}' - \pi/6\right) + 0.24 \cos\left(2\bar{H}'\right) + 0.32 \cos\left(3\bar{H}' + \pi/30\right) - 0.20 \cos\left(4\bar{H}' - 21\pi/60\right)$$

$$S_L = 1 + \frac{0.015 \left(\bar{L} - 50\right)^2}{\sqrt{20 + \left(\bar{L} - 50\right)^2}}$$

$$S_C = 1 + 0.045 \bar{C}'$$

$$S_H = 1 + 0.015 \bar{C}' T$$

$$R_T = -2 \sqrt{\frac{\bar{C}'^7}{\bar{C}'^7 + 25^7}} \sin\left[\frac{\pi}{6} \exp\left(-\left[\frac{\bar{H}' - 275^\circ}{25}\right]^2\right)\right]$$

2.4.5 CMC 1: c (1984)

In 1984, the Colour Measurement Committee of the Society of Dyers and Colourists defined a difference measure, also based on the L*C*h colour model. Named after the developing committee, their metric is called **CMC 1: c**. The quasimetric has two parameters: lightness (l) and chroma (c), allowing the users to weight the difference based on the ratio of l: c that is deemed appropriate for the application. Commonly-used values are 2:1 [18] for acceptability and 1:1 for the threshold of imperceptibility.

The distance of a colour (L_2^*, C_2^*, h_2)

$$T = \begin{cases} 0.56 + |0.2 \cos(h_1 + 168^\circ)| \\ 0.36 + |0.4 \cos(h_1)| \end{cases}$$

to a reference (L_1^*, C_1^*, h_1) is:

$$\Delta E_{CMC}^* = \sqrt{\left(\frac{L_2^* - L_1^*}{l S_L}\right)^2 + \left(\frac{C_2^* - C_1^*}{c S_C}\right)^2 + \left(\frac{\Delta H^*}{S_H}\right)^2}$$

$$S_L = \begin{cases} 0.511 & L_1^* < 16 \\ \frac{0.040975 L_1^*}{1 + 0.01765 L_1^*} & L_1^* \geq 16 \end{cases} \quad S_C = \frac{0.0638 C_1^*}{1 + 0.0131 C_1^*} + 0.638 \quad S_H = S_C (FT + 1 - F)$$

$$T = \begin{cases} 0.56 + |0.2 \cos(h_1 + 168^\circ)| & 164^\circ \leq h_1 \leq 345^\circ \\ 0.36 + |0.4 \cos(h_1 + 35^\circ)| & \text{otherwise} \end{cases}$$

$$F = \sqrt{\frac{C_1^{*4}}{C_1^{*4} + 1900}}$$

CMC 1:c is designed to be used with D65 and the CIE Supplementary Observer [19].

2.4.6 Tolerance

Tolerancing concerns the question "What is a set of colours that are imperceptibly/acceptably close to a given reference?" If the distance measure is perceptually uniform, then the answer is simply "the set of points whose distance to the reference is less than the just-noticeable-difference (JND) threshold." This requires a perceptually uniform metric in order for the threshold to be constant throughout the gamut (range of colours). Otherwise, the threshold will be a function of the reference colour—useless as an objective, practical guide.

In the CIE 1931 colour space, for example, the tolerance contours are defined by the MacAdam ellipse, which holds L* (lightness) fixed. As can be observed on the diagram on the right, the ellipses denoting the tolerance contours vary in size. It is partly due to this non-uniformity that lead to the creation of CIELUV and CIELAB.

More generally, if the lightness is allowed to vary, then we find the tolerance set to be ellipsoidal. Increasing the weighting factor in the aforementioned distance expressions has the effect of increasing the size of the ellipsoid along the respective axis [20]. Turgay Celik and Tardi Tjahjadi [21] presented an effective unsupervised colour image segmentation algorithm which uses multiscale edge information and spatial colour content. The segmentation of homogeneous regions is obtained using region growing followed by region merging in the CIE L*a*b* colour space.

2.4.7 Delta E Differences and Tolerances

The difference between two colour samples is often expressed as Delta E, also called DE, or ΔE. 'Δ' is the Greek letter for 'D'. This can be used in quality control to show whether a printed sample, such as a colour swatch or proof, is in tolerance with a reference sample or industry standard. The difference between the L*, a* and b* values between the reference and print will be shown as Delta E (ΔE). The resulting Delta E number will show how far apart visually the two samples are in the colour 'sphere'.

Customers may specify that their contract proofs must have tolerances within ΔE 2.0 for example. Different tolerances may be specified for greys and primary colours. A value of less than 2 is common for greys and less than 5 for primary CMYK and overprints. This is somewhat contentious however. Proofing RIPs sometimes have verification software to check a proof against a standard scale, such as an Ugra/Fogra Media Wedge, using a spectrophotometer. Various software applications are available to check colour swatches and spot colours, proofs, and printed sheets.

Delta E displays the difference as a single value for colour and lightness. ΔE values of 4 and over will normally be visible to the average person, while those of 2 and over may be visible to an experienced observer. Note that there are several subtly different variations of Delta E: CIE 1976, 1994, 2000, cmc delta e [22].

III. Color-Based Segmentation Using Proposed Clustering Technique

The proposed approach performs clustering of color space. A particle consists of K cluster centroids representing L*a*b* color triplets. The basic aim is to segment colors in an automated fashion using the L*a*b* color space and K-means clustering. The entire process can be summarized in following steps

Step 1: Read the image.

Read the image from mother source which is in .JPEG format, which is a fused image.

Step 2: For colour separation of an image apply the De-correlation stretching.

Step 3: Convert Image from RGB Color Space to L*a*b* Color Space. How many colors do we see in the image if we ignore variations in brightness? There are three colors: white, blue, and pink. We can easily visually distinguish these colors from one another.

The L*a*b* color space (also known as CIELAB or CIE L*a*b*) enables us to quantify these visual differences. The L*a*b* color space is derived from the CIE XYZ tristimulus values. The L*a*b* space consists of a luminosity layer 'L*', chromaticity-layer 'a*' indicating where color falls along the red-green axis, and chromaticity-layer 'b*' indicating where the color falls along the blue-yellow axis. All of the color information is in the 'a*' and 'b*' layers. We can measure the difference between two colors using the Euclidean distance metric. Convert the image to L*a*b* color space.

Step 4: Classify the Colors in 'a*b*' Space Using K-Means Clustering.

Clustering is a way to separate groups of objects. K-means clustering treats each object as having a location in space. It finds partitions such that objects within each cluster are as close to each other as possible, and as far from objects in other clusters as possible. K-means clustering requires that you specify the number of clusters to be partitioned and a distance metric to quantify how close two objects are to each other. Since the color information exists in the 'a*b*' space, your objects are pixels with 'a*' and 'b*' values. Use K-means to cluster the objects into three clusters using the Euclidean distance metric.

Step 5: Label Every Pixel in the Image using the results from K-MEANS.

For every object in our input, K-means returns an index corresponding to a cluster. Label every pixel in the image with its cluster index.

Step 6: Create Images that Segment the Image by Color.

Using pixel labels, we have to separate objects in image by Color.

Step 7: Segment the Nuclei into a Separate Image.

3.1 Proposed Clustering algorithm

Proposed clustering algorithm is under the category of Squared Error-Based Clustering (Vector Quantization) and it is also under the category of crisp clustering or hard clustering. Proposed algorithm is very simple and can be easily implemented in solving many practical problems. Proposed algorithm is ideally suitable for biomedical image segmentation since the number of clusters (k) is usually known for images of particular regions of human anatomy. Steps of the proposed clustering algorithm are given below:

1) Choose k cluster centers to coincide with k randomly chosen patterns inside the hyper volume containing the pattern set (C).

2) Assign each pattern to the closest cluster center. i.e. ($C_i, i=1,2,\dots,C$)

3) Recompute the cluster centers using the current cluster memberships. (U):

$$u_{ij} = \begin{cases} 1, & \text{if } \|x_j - C_i\|^2 \leq \|x_j - C_k\|^2, \text{ for each } k \neq i \\ 0, & \text{otherwise} \end{cases}$$

4)

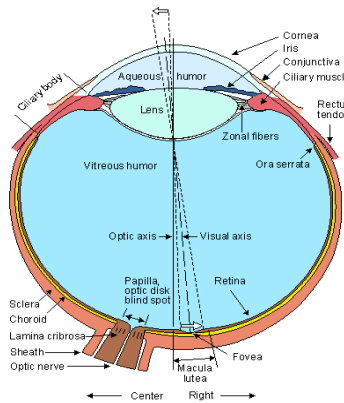
5) If convergence criterion is not met, go to step 2 with new cluster centers by the following equation, i.e. minimal decrease in squared error:

$$c_i = \frac{i}{G_i} \sum_{k, X_k \in G_i} X_k$$

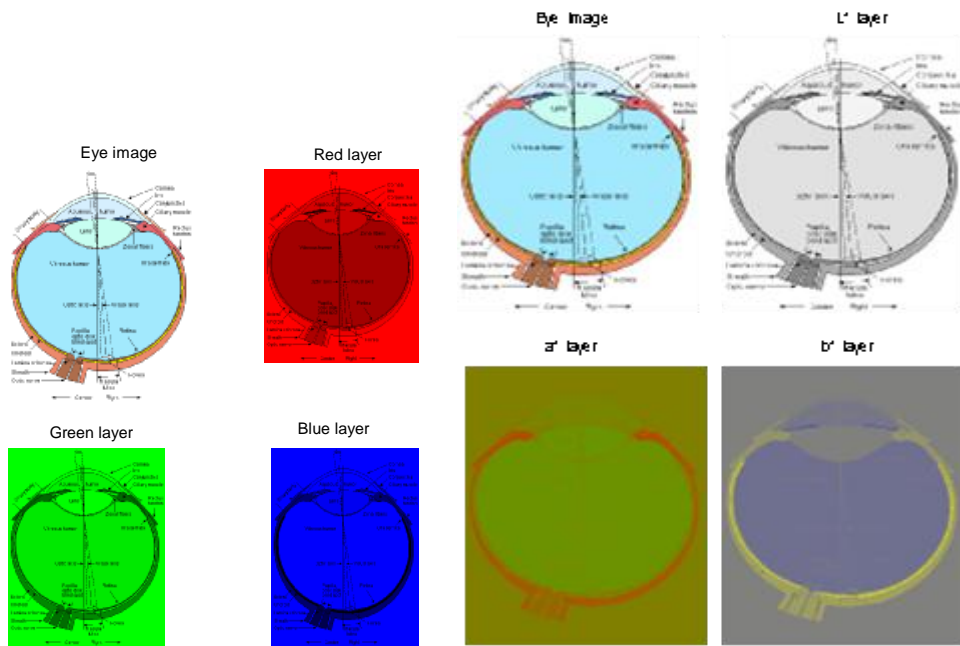
Where, $|G_i|$ is the size of G_i or $|G_i| = \sum_{j=1}^n u_{ij}$

IV. Results and Discussion

After the conversion of image into L*a*b* color space, segmentation algorithm is applied. Figure 3 shows the results of Eye image with (a) Original image (b) Result using RGB color space (c) Result using L*a*b* color space (d) Histogram. Histogram represents the standard deviation and variance. Figure 4 shows the results of Human Eye image with (a) Original image (b) Result using RGB color space (c) Result using L*a*b* color space. Figure 5 shows the results of Human Brain image with (a) Original image (b) Result using RGB color space (c) Result using L*a*b* color space (d) Brain segmented cavity (e) Brain segmented object (Temporal Lobe) with proposed COLOR CLUSTERING Technique (f) Histogram (g) color classification scatter plot representation of the segmented pixels in L*a*b* color space. Here temporal lobe is segmented successfully from brain image. Figure 6 shows the results of Human Heart image with (a) Original image (b), (c) and (d) Heart image segmented objects with proposed COLOR CLUSTERING Technique (e) color classification scatter plot representation of the segmented pixels in L*a*b* color space. Scatter plot represents clusters of color pixels in the segmented image. Here various heart vessels and heart chambers are segmented from heart image. Figure 7 shows the results of Matlab standard peppers image for two different Region of interest (ROI) (a) first ROI having $\Delta E \leq 30.9$ or >30.9 (b) second ROI having $\Delta E \leq 54.3$ or >54.3 . Figure 7 represents the complete steps to obtain segmentation with selection of object of interest (Region of Interest (ROI)), L*a*b* representation, their histograms and segmented results with matching colors or not matching colors.

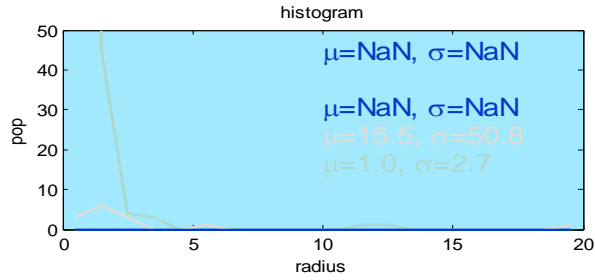


(a)

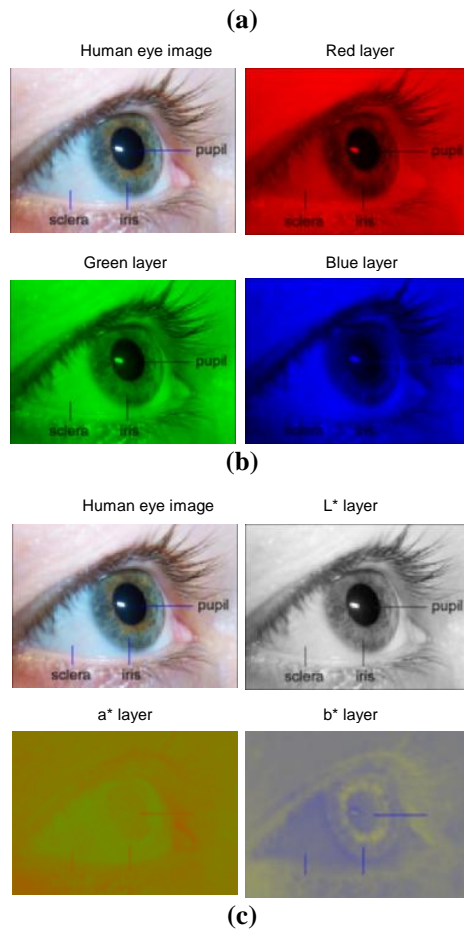


(b)

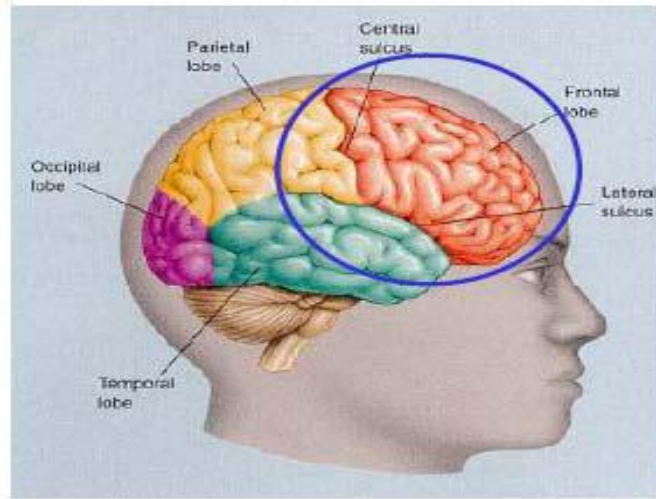
(c)



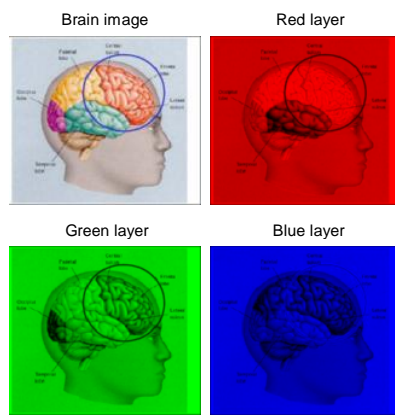
(d)
Figure 3: Results of Eye image (a) Original image (b) Result using RGB color space (c) Result using $L^*a^*b^*$ color space (d) Histogram



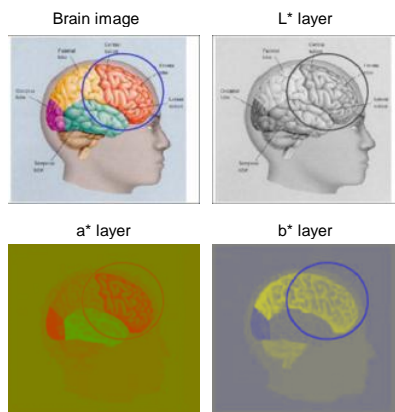
(c)
Figure 4: Results of Human Eye image (a) Original image (b) Result using RGB color space (c) Result using $L^*a^*b^*$ color space



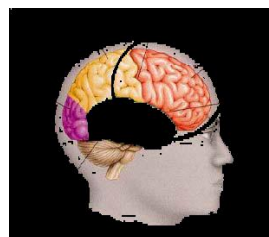
(a)



(b)



(c)



(d)

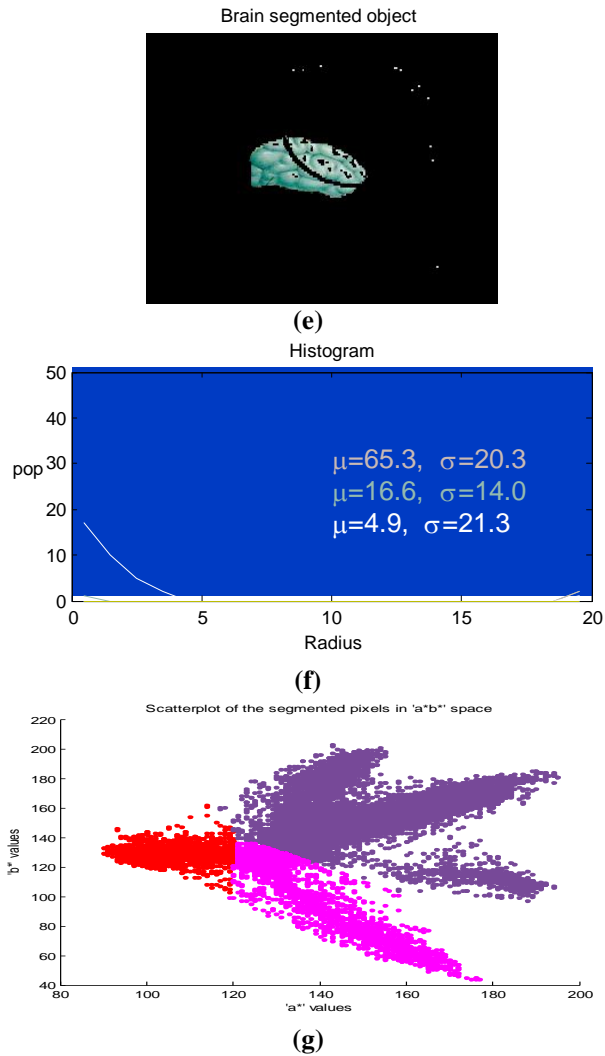
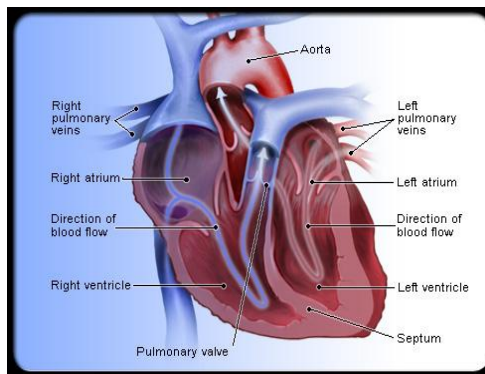
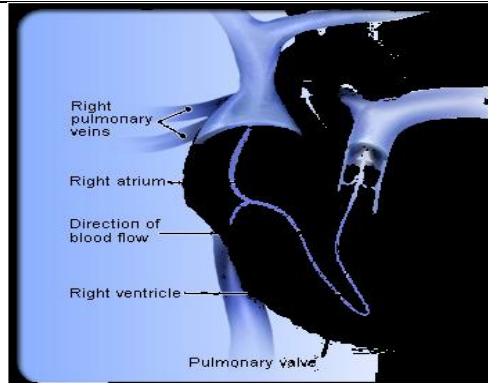


Figure 5: Results of Human Brain image (a) Original image (b) Result using RGB color space (c) Result using $L^*a^*b^*$ color space (d) Brain segmented cavity (e) Brain segmented object (Temporal Lobe) with proposed COLOR CLUSTERING Technique (f) Histogram (g) color classification scatter plot representation of the segmented pixels in $L^*a^*b^*$ color space.



(a)



(b)



(c)



(d)

(e)

Figure 6: Results of Human Heart image (a) Original image (b) (c) (d) Heart image segmented objects with proposed COLOR CLUSTERING Technique (e) color classification scatter plot representation of the segmented pixels in $L^*a^*b^*$ color space.

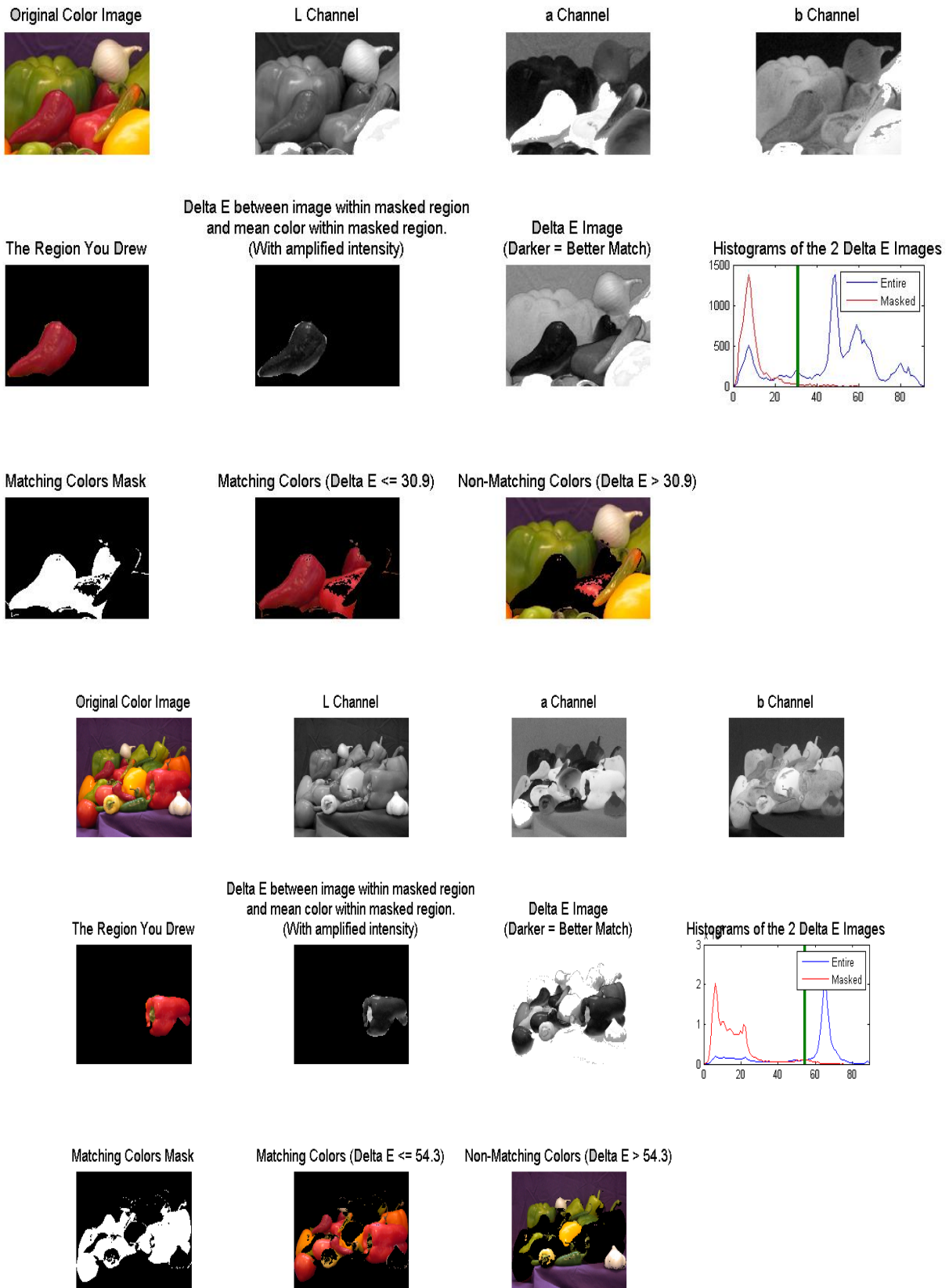


Figure 7: Results of Matlab standard peppers image for two different Region of interest (ROI) (a) first ROI having Delta E ≤ 30.9 or > 30.9 (b) second ROI having Delta E ≤ 54.3 or > 54.3

V. Conclusion

A novel approach employing color clustering image segmentation using L*a*b* color space on biomedical images is proposed. Color clustering image segmentation algorithm, segments the important object information from images. The effectiveness of the proposed method is tested by conducting two sets of experiments out of which one is meant for medical images segmentation and one for standard images from Mat Lab software.

References

- [1] Hunter, Richard Sewall (July 1948). "photoelectric color-difference meter". *Josa* 38 (7): 661. (Proceedings of the winter meeting of the optical society of America)
- [2] Hunter, Richard Sewall (December 1948). "Accuracy, precision, and stability of new photo-electric color-difference meter". *Josa* 38 (12): 1094. (Proceedings of the thirty-third annual meeting of the optical society of America)
- [3] International color consortium, specification icc.1:2004-10 (profile version 4.2.0.0) image technology colour management — architecture, profile format, and data structure, (2006).
- [4] Margulis, Dan (2006). *Photoshop lab color: the canyon conundrum and other adventures in the most powerful color space*. Berkeley, Calif.: London: peachpit; Pearson education. ISBN 0321356780.
- [5] Brainard, David h. (2003). "color appearance and color difference specification". In shevell, Steven k. *The science of color* (2 Ed.). Elsevier. p. 206. ISBN 0444512519.
- [6] Fairchild, mark d. (2005). "Color and image appearance models". *Color appearance models*. John Wiley and sons. p. 340. ISBN 0470012161.
- [7] Jain, Anil K. (1989). *Fundamentals of digital image processing*. New Jersey, United States of America: prentice hall. pp. 68, 71, 73. isbn 0-13-336165-9.
- [8] Janos schanda (2007). *colorimetry*. Wiley-interscience. p. 61. isbn 9780470049044.
- [9] Hunter labs (1996). "Hunter lab color scale". *Insight on color* 8 9 (august 1–15, 1996). Reston, VA, USA: hunter associates laboratories.
- [10] Adams, e.q. (1942). "x-z planes in the 1931 i.c.i. system of colorimetry". *Josa* 32 (3): 168–173. doi:10.1364/josa.32.000168.
- [11] Gaurav Sharma (2003). *Digital Color Imaging Handbook* (1.7.2 Ed.). CRC Press. ISBN 084930900X. <http://books.google.com/?id=OxIBqY67r10C&pg=PA31&vq=1.42&dq=jnd+gaurav+sharma>.
- [12] "Delta E: The Color Difference". *Colorwiki.com*. http://www.colorwiki.com/wiki/Delta_E:The_Color_Difference. Retrieved 2009-04-16.
- [13] Bruce Justin Lind bloom. "Delta E (CIE 1994)". *Brucelindbloom.com*. http://www.brucelindbloom.com/Eqn_DeltaE_CIE94.html. Retrieved 2011-03-23.
- [14] "Colour Difference Software by David Heggie". *Colorpro.com*. 1995-12-19. <http://www.colorpro.com/info/software/heggie.html>. Retrieved 2009-04-16.
- [15] "CIE 1976 L*a*b* Colour space draft standard", http://www.physics.kee.hu/cie/newcie/nc/DS014-4_3.pdf. Retrieved 2011-03-23.
- [16] Sharma, Gaurav; Wencheng Wu, Edul N. Dalal (2005). "The CIEDE2000 color-difference formula: Implementation notes, supplementary test data, and mathematical observations". *Color Research & Applications* (Wiley Interscience) 30(1): 21–30. doi:10.1002/col.20070. <http://www.ece.rochester.edu/~gsharma/ciede2000/ciede2000noteCRNA.pdf>.
- [17] Bruce Justin Lind bloom. "Delta E (CIE 2000)". *Brucelindbloom.com*. http://www.brucelindbloom.com/Eqn_DeltaE_CIE2000.html. Retrieved 2009-04-16.
- [18] Bruce Justin Lind bloom. "Delta E (CMC)". *Brucelindbloom.com*. http://www.brucelindbloom.com/Eqn_DeltaE_CMC.html. Retrieved 2009-04-16.
- [19] http://www.xrite.com/documents/literature/en/L10-024_Color_Tolerance_en.pdf
- [20] Turgay Celik, Tardi Tjahjadi, Unsupervised colour image segmentation using dual-tree complex wavelet transforms, *Computer Vision and Image Understanding* 114 (2010) 813–826.
- [21] H.-D. Cheng and Y. Sun, "A hierarchical approach to color image segmentation using homogeneity," *IEEE Transactions on Image Processing*, vol. 9, no. 12, pp. 2071–2082, 2000.
- [22] <http://en.wikipedia.org/wiki/>



Janak B. Patel (born in 1971) received B.E. (Electronics & Communication Engg from L.D. College of Engg. Ahmedabad, affiliated with Gujarat University and M.E. (Electronics Communication & System Engg.) in 2000 from Dharmsinh Desai Institute of Technology, Nadiad, affiliated with Gujarat University. He is Asst. Professor at L.D.R.P. Institute of Technology & Research, Gandhinagar, and Gujarat. Currently, he is pursuing his Ph.D. program at Indian Institute of Technology, Roorkee under quality improvement program of AICTE, India. His research interest includes digital signal processing, image processing, bio-medical signal and image processing. He has 7 years of industrial and 12 years of teaching experience at Engineering College. He taught many subjects in EC, CS and IT disciplines. He is a life member of CSI, ISTE & IETE.



R.S. Anand received B.E., M.E. and Ph.D. in Electrical Engg. from University of Roorkee (Indian Institute of Technology, Roorkee) in 1985, 1987 and 1992, respectively. He is a professor at Indian Institute of Technology, Roorkee. He has published more than 100 research papers in the area of image processing and signal processing. He has also supervised 10 PhDs, 60 M.Tech.s and also organized conferences and workshops. His research areas are biomedical signals and image processing and ultrasonic application in non-destructive evaluation and medical diagnosis. He is a life member of Ultrasonic Society of India.